Soft x-ray absorption spectroscopy study of electrochemically formed passive layers on AISI 304 and 316L stainless steels

M. F. López, A. Gutiérrez, C. L. Torres, and J. M. Bastidas
Centro Nacional de Investigaciones Metalúrgicas (CSIC), Avda. Gregorio del Amo 8, Madrid 28040, Spain

(Received 19 January 1998; accepted 19 July 1998)

The structure and composition of passive films electrochemically formed on AISI 304 and 316L stainless steels in a chloride-containing solution have been studied by soft x-ray absorption spectroscopy. Soft x-ray absorption spectra were taken at the oxygen *1s* edge and at the transition metals (Cr, Fe, Ni) *2p* edges, making it possible to determine the main contributions to the passive film's composition. The soft x-ray absorption spectra at the Cr *2p* edges indicate that in all cases the passive film is mainly formed by Cr_2O_3. Spectra at the Fe and Ni *2p* edges exhibit no significant contribution of Ni and Fe oxides to the passive layer composition. However, differences in spectral shape with respect to metallic Ni and Fe suggest the presence of a small amount of hydroxides, which is maximum for the AISI 304 stainless steel polarized at the lowest scan rate. The spectra at the O *1s* edges confirm the results obtained at the transition metal edges.

I. INTRODUCTION

Stainless steels are materials of great interest in technological applications. One of their characteristic properties is the high corrosion resistance provided by the presence of a passive layer formed on their surface. This surface passive layer improves the corrosion resistance of the material, serving as a protective barrier against the aggressive environment. Consequently, the chemical composition of the passive films formed on stainless steels has been the subject of many research studies. The techniques mostly used to perform this surface investigation have been x-ray photoelectron spectroscopy (XPS) and Auger electron spectroscopy (AES).[1–10] In general, these studies revealed that the passive film is enriched in Cr close to the alloy, whereas appreciable amounts of hydroxides and water are concentrated at the outermost layers of the film.

Surface sensitive techniques have become valuable tools to study different chemical compounds formed on metal surfaces during passivation. The sampling depth of XPS and AES is about 20 Å.[11] X-ray absorption spectroscopy (XAS) is a core level spectroscopy that excites an electron from a core state to an empty state. The absorption cross section can be measured by detecting electrons which escape from the surface as a result of the decay of the core hole. The Auger electron yield method of XAS is used when the energy of the outgoing electrons is selected; i.e., the intensity of a specific Auger decay channel of the core hole is measured. The probe depth of this method is ≈ 20 Å, which is rather surface sensitive, similar to the XPS technique. However, when the energy of the excited electrons is not selected and simply all escaping electrons are counted, we deal with the total electron yield (TEY) mode. In this detection method, the signal is dominated by secondary electrons which are created in the cascade process of the Auger decay electrons. A rough estimate for the probing depth is of the order of 70–100 Å for the transition metal *2p* edges,[12,13] i.e., larger than that of XPS. XAS is an element selective technique because the core level binding energy is specific to a certain chemical element. This technique can give information on the chemical properties such as valency.[14–20]

The aim of the present study is to investigate the chemical composition of two stainless steels, AISI 304 and 316L, using soft x-ray absorption spectroscopy. Applying this technique at the O *1s* edge and at the transition metals *2p* edges in TEY mode, it will be possible to characterize deeper the electrochemically formed passive layers on the surface of these materials. The samples were measured after performing anodic polarization curves up to two different polarization potentials. Two different scan rates were used to study the influence of the sweep rate on the composition of the passive layer. For comparative purposes, unpolarized samples, i.e., samples without any electrolyte immersion or polarization measurements, were also investigated.

II. EXPERIMENTAL

The two austenitic stainless steels (SS) investigated are AISI 304 SS and 316L SS. The chemical composition of AISI 304 SS is (wt%) 19.7 Cr, 9.4 Ni, 1.7 Mn, 0.28 Si, 0.036 C, 0.003 S, 0.022 P, and the remainder is Fe. The chemical composition of AISI 316L SS is (wt%) 17.1 Cr, 10.7 Ni, 2.2 Mo, 1.2 Mn, 0.4 Si, 0.019 C, 0.018 S, 0.02 P, and the remainder is

Fe. Before testing, the samples (10 × 10 × 4 mm) were embedded in cold epoxy resin and mechanically polished with successive SiC papers of 120, 400, and 600 grades, followed with alumina and, finally, diamond paste of 1 μm grain size.

Anodic polarization curves were carried out at room temperature using as electrolyte 500 ml of a 5% NaCl aqueous solution (pH $\approx$ 8) prepared from reagent grade NaCl and distilled water. The electrochemical cell used was similar to the ASTM G-5 standard. To simulate service conditions, no purge gas was employed.

Anodic polarization curves were performed after 30 min exposure to a 5% NaCl electrolyte, starting at the open-circuit potential. An EG&G PARC 273A potentiostat was used in the three-electrode configuration. A saturated calomel electrode (SCE) was used as reference and a platinum wire as counter electrode. The 1 cm^2 AISI 304 and 316L SS specimens were the working electrodes. Two sweep rates were used: 0.16 and 5.0 mV s^{-1}.

After polarization tests, the samples were extracted from the electrochemical cell, rinsed in distilled water, removed from the epoxy resin with special care not to damage the surface to be analyzed, and stored in a desiccator until they were placed in the ultrahigh vacuum chamber (UHV) for the XAS measurements.

XAS measurements were performed on the AISI 304 and 316L SS samples polarized at the two different sweep rates, 0.16 and 5.0 mV s^{-1}. Additionally, for each polarized SS sample two different regions were studied: (a) the passive region, which corresponds to samples labeled "A" and "C," and (b) the pitting region, which corresponds to samples labeled "B" and "D." Figure 1 exhibits the anodic polarization curves at the two investigated scan rates, 0.16 and 5.0 mV s^{-1}, for the AISI 304 and 316L SS sample immersed in a 5% NaCl electrolyte. The different regions studied are indicated in Fig. 1. As can be seen, at low anodic polarization the current density increases with increasing anodic potential. In this region, the anodic current density corresponds only to the dissolution of the film covering the material. After that, the passive state is achieved. Therefore, the material shows a passive region with low current density until the breakdown potential is reached. At this potential, the current density drastically increases, which is attributed to the activation of a local corrosion process. Samples B and D were chosen at the pitting region, i.e., after the breakdown potential was achieved. The curves show that by increasing the scan rate the breakdown potential also increases and the passivity region becomes larger.

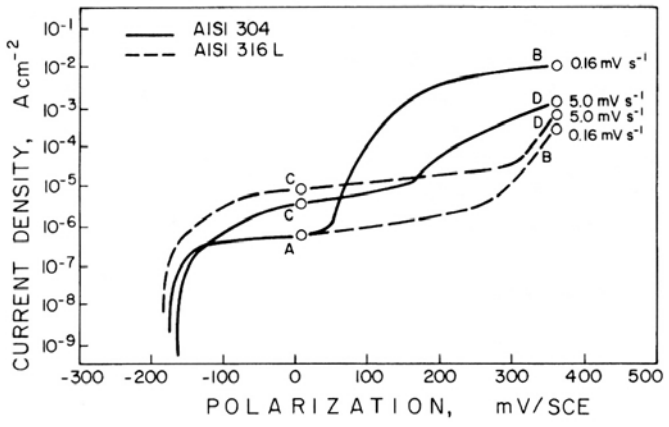

FIG. 1. Typical anodic polarization curves of AISI 304 and 316L SS immersed in a 5% NaCl solution at two scan rates, 0.16 and 5.0 mV s^{-1}. The points labeled A, B, C, and D were the different regions studied by XAS.

For comparative purposes and as reference materials, the following samples were also studied: (a) unpolarized AISI 304 and 316L SS samples with the same surface preparation as described above for polarized samples; (b) Fe, Cr, and Ni pure metal samples, in the form of polycrystalline material; these samples were scraped *in situ* in the UHV chamber with a diamond file to measure the clean metal surfaces; and (c) FeO, NiO, oxidized Fe, and oxidized Cr samples. Both Fe and Cr oxidized samples were produced by air exposure of the metal samples, generating spontaneously a native oxide layer on each sample surface. FeO and NiO samples were pressed pellets of FeO and NiO powders, respectively, and were scraped *in situ* in the UHV chamber with a diamond file to remove surface contaminants.

The XAS measurements were carried out at the SX700/II soft x-ray monochromator operated by the Freie Universität Berlin at the Berliner Elektronenspeicherring für Synchrotronstrahlung (BESSY). XAS spectra were obtained at the *2p* absorption thresholds of the transition metals (Cr, Fe, and Ni) and at the *1s* absorption threshold of oxygen by recording the total yield of secondary electrons from the sample surfaces, i.e., in TEY mode. The base pressure in the UHV chamber during the measurements was better than 2×10^{-10} mbar.

III. RESULTS AND DISCUSSION

The Cr *2p* soft x-ray absorption spectra of unpolarized AISI 316L SS, the four polarized SS samples (A, B, C, D), oxidized Cr, and Cr metal are shown in Fig. 2. The spectra consist of two multiplets, which are separated, to a first approximation, by the spin-orbit splitting of the Cr *2p* core hole. The spectra of the AISI 316L SS samples correspond clearly to Cr_2O_3, as can be concluded by comparing with the Cr_2O_3 spectrum of previous works.[21] The typical shape of the Cr_2O_3 soft x-ray absorption spectrum exhibits, in the $2p_{3/2}$ region, a main peak at $\approx$ 577 eV, marked in Fig. 2 by a vertical line, and a distinctive shoulder located at $\approx$ 575.5 eV.

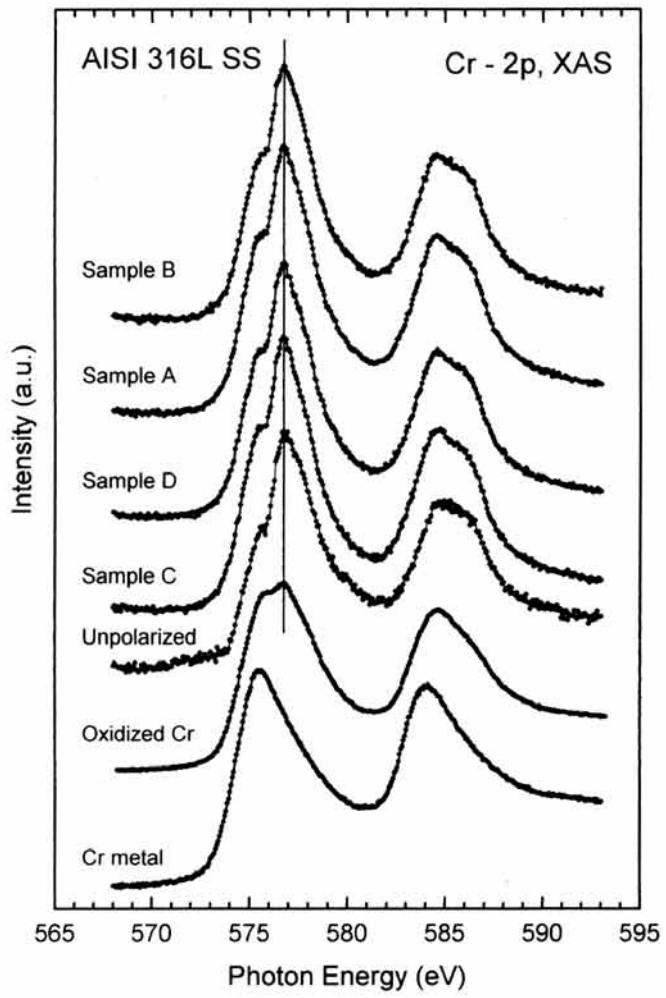

FIG. 2. Cr *2p* soft x-ray absorption spectra for the four polarized AISI 316L SS, the unpolarized AISI 316L SS, oxidized Cr, and Cr metal samples. The solid lines through the data points serve as a guide to the eyes.

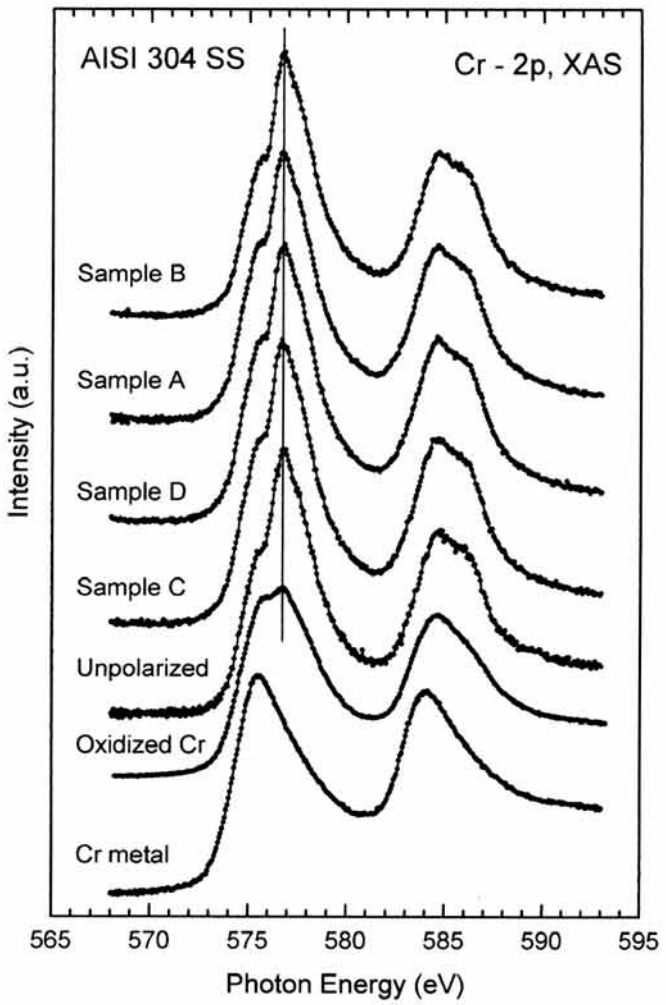

FIG. 3. Cr *2p* soft x-ray absorption spectra for the four polarized AISI 304 SS and the unpolarized AISI 304 SS, oxidized Cr, and Cr metal samples. The solid lines through the data points serve as a guide to the eyes.

The spectrum of Cr metal has a different shape from that of Cr_2O_3 with a main peak located at ≈ 575.5 eV. The oxidized Cr spectrum that corresponds to the native oxide film is a mixture of metallic chromium and Cr_2O_3. As the metallic contribution increases, the intensity of the shoulder at ≈ 575.5 eV also increases. For the same photon energy, the probe depth of this technique is the same. Therefore, since the metallic component in the oxidized Cr sample is higher than in the AISI 316L SS samples, it can be concluded that the passive layer in oxidized Cr is narrower than in the SS samples.

For the case of AISI 304 SS samples, the Cr *2p* spectra are shown in Fig. 3 where the same behavior as in the AISI 316L SS case is observed. All AISI 304 SS samples, polarized and unpolarized, exhibit the typical spectrum of Cr_2O_3.[21] Therefore, the Cr *2p* spectra indicate that the chemical state of chromium in the passive layer is mainly Cr_2O_3. No metallic contribution is observed, which would be indicated by an intensity increase of the shoulder at ≈ 575.5 eV, contrary to the case of oxidized Cr, indicating a thicker passive layer for the SS samples, as observed for the AISI 316L SS samples.

Figure 4 exhibits Fe *2p* soft x-ray absorption spectra of AISI 316L SS samples, polarized and unpolarized, Fe metal and FeO. On the other hand, the Fe *2p* soft x-ray absorption spectra of AISI 304 SS samples, polarized and unpolarized, are shown in Fig. 5. All spectra present two broad multiplets separated by the spin-orbit splitting of the Fe *2p* core hole. The SS spectra are similar to Fe metal although some differences can be observed. In general, the spectra of both AISI 316L and 304 SS samples show a $2p_{3/2}$ peak narrower than in the pure metal case. This effect can be related to the narrowing of the metal *3d* bands in the alloys as compared to the pure metal.[22] Another difference of the SS spectra with the Fe metal spectrum is the presence of a small shoulder marked by a vertical arrow in Fig. 5 at a photon

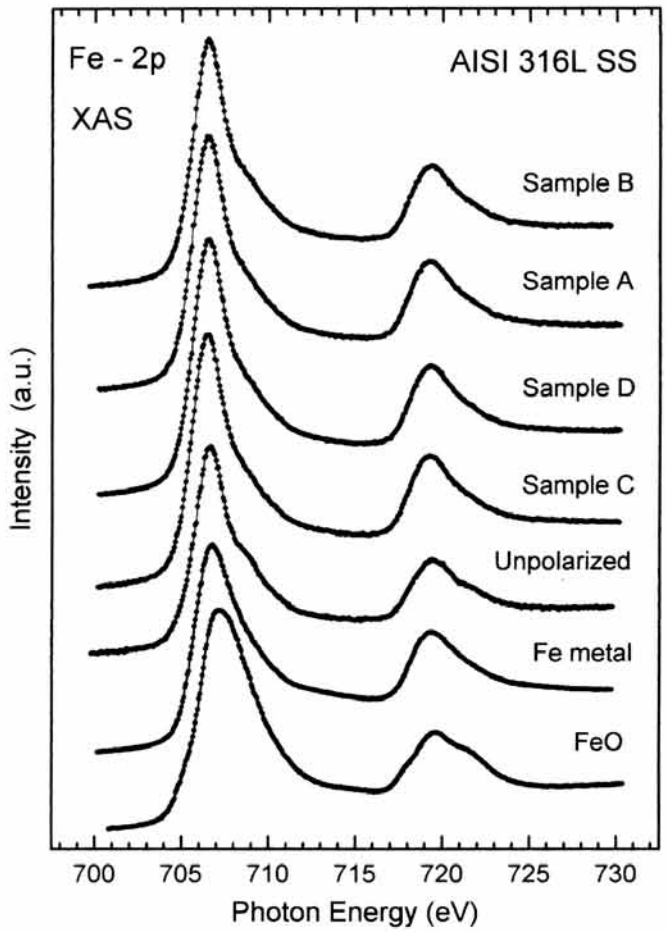

FIG. 4. Fe $2p$ soft x-ray absorption spectra for the four polarized AISI 316L SS, the unpolarized AISI 316L SS, Fe metal, and FeO samples. The solid line through the data points serves as an eye line.

energy of ≈ 708.5 eV. These differences between SS samples and Fe metal cannot be attributed to the presence of FeO because the FeO spectrum exhibits broader $2p_{3/2}$ and $2p_{1/2}$ bands with a well-defined shoulder at ≈ 721 eV. Additionally, by comparison of the SS Fe $2p$ spectra with Fe_3O_4 and Fe_2O_3 spectra from previous works,[21] it can be concluded that the observed differences between SS and Fe metal cannot be attributed to either of these iron oxides. One possibility is that the differences between the SS spectra and the Fe metal spectrum are associated with the presence of hydroxide compounds or hydrated molecules in the SS samples. For the AISI 304 SS sample B, the differences with Fe metal are more evident. The shoulder at ≈ 708.5 eV is slightly more intense and the $2p_{3/2}$ peak is narrower than in the other SS samples. Samples A and C were obtained at the passive region, where the passive layer has no damage. Samples B and D were obtained in the pitting region, where local corrosion is present. Sample D showed a lower number of pits than sample B; slower scan rates produce a more intense attack. This can explain the higher presence of hydroxide compounds in the sample B as compared to the other polarized samples. Concerning the unpolarized samples, the AISI 316L SS spectrum also exhibits the shoulder at ≈ 708.5 eV slightly more intense than other SS samples. Besides, for this sample a small shoulder at ≈ 721 eV in the $2p_{1/2}$ region is observed which is similar to that of FeO, indicating the presence of FeO. Therefore, the unpolarized 316L SS passive layer, which is formed not electrochemically but spontaneously in contact with air, is composed mainly of Cr_2O_3, but with a slightly higher amount of Fe hydroxides and FeO than the other SS samples. The presence of Fe hydroxides and FeO in this case can be justified by the different nature of the passive layer in this case as compared with polarized samples. Because of the contact with air and the low thickness of the Cr_2O_3 protective layer, the initial reaction of Fe with the atmosphere to form small amounts of Fe hydroxides and FeO may occur even though the main composition of the passive layer is Cr_2O_3. However, the Fe $2p$ spectrum of unpolarized 304 SS exhibits a different behavior, with a lower amount of Fe hydroxides and FeO. A possible explanation for this different behavior could be the differences in the chemical composition of both

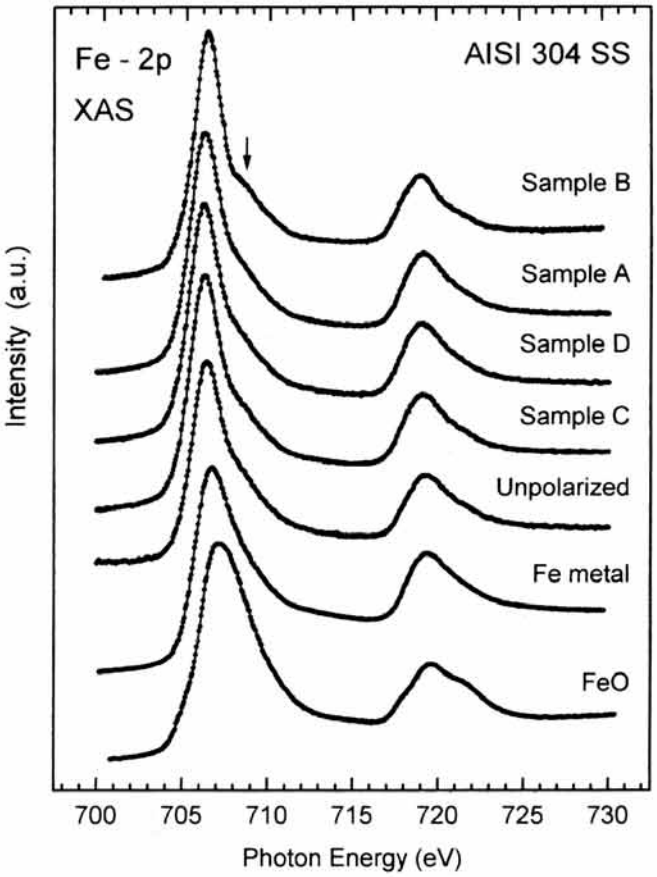

FIG. 5. Fe $2p$ soft x-ray absorption spectra for the four polarized AISI 304 SS and the unpolarized AISI 304 SS, Fe metal, and FeO samples. The solid lines through the data points serve as a guide to the eyes.

materials. Sample 316L SS has a lower proportion of Cr in the material, 17.1 wt%, than the 304 SS, 19.7 wt%. This lower Cr content in the case of the 316L SS sample could be the reason for the slightly higher amount of Fe hydroxides and FeO in the passive layer as compared with the 304 sample. In any case, all Fe *2p* spectra of the SS polarized and unpolarized samples exhibit high similarity with the Fe *2p* spectrum of Fe metal. Since the probing depth of XAS in TEY is larger than the thickness of the passive layer of SS, the influence of the metallic contribution from the substrate was expected in the Fe *2p* spectra. This result, however, seems to be in disagreement with the Cr *2p* SS spectra where no metallic Cr contribution was observed. From the Cr *2p* spectra and from the previous findings in the literature, it is known that the main component of the passive layer of the SS is Cr_2O_3. With the XAS spectra we have observed almost no metallic Cr *2p* absorption. However, we have to take into account that the Cr content in the alloy is much lower than the Fe content. Therefore, the XAS Cr *2p* SS spectra exhibit the structure of Cr_2O_3 with only a small contribution of metallic Cr from the substrate. The XAS Fe *2p* SS spectra show, however, the structures of Fe metal with some small contribution of hydroxides from the surface.

The Ni *2p* spectra of the unpolarized and polarized AISI 316L SS samples together with Ni metal and NiO samples are shown in Fig. 6. All SS spectra show a high similarity to the spectrum of clean Ni metal. The satellite located at ≈ 859 eV, which is characteristic of metallic Ni, is present in all SS spectra.

The Ni *2p* spectra of unpolarized and polarized AISI 304 SS samples are shown in Fig. 7. Also in this case all spectra are rather similar to metallic Ni.

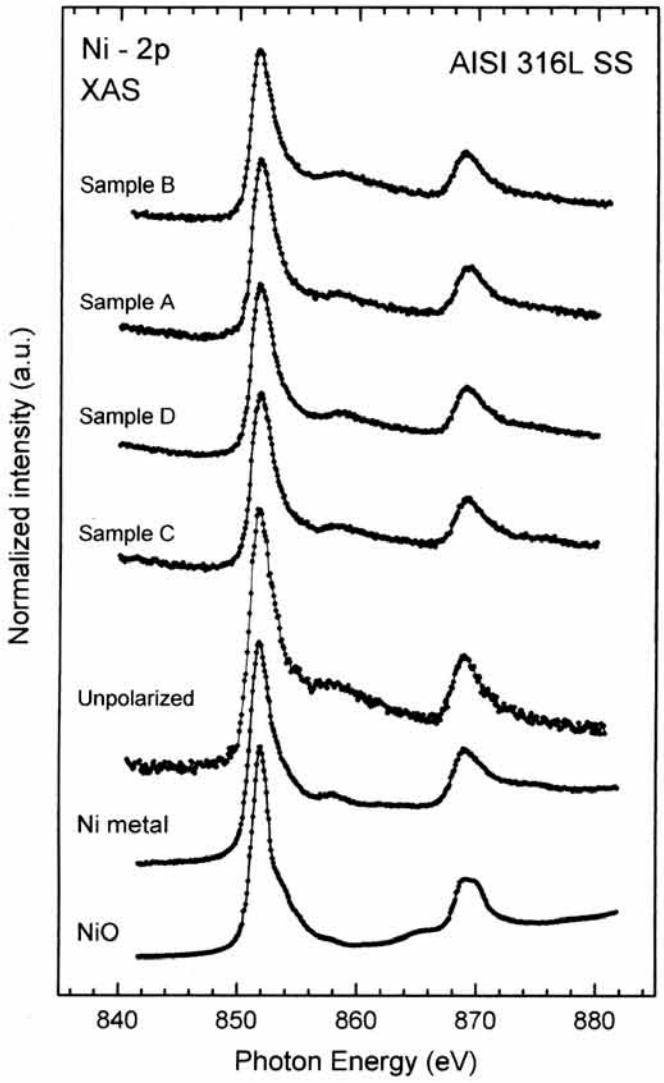

FIG. 6. Ni *2p* soft x-ray absorption spectra for the four polarized AISI 316L SS, the unpolarized AISI 316L SS, Ni metal, and NiO samples. The solid lines through the data points serve as a guide to the eyes.

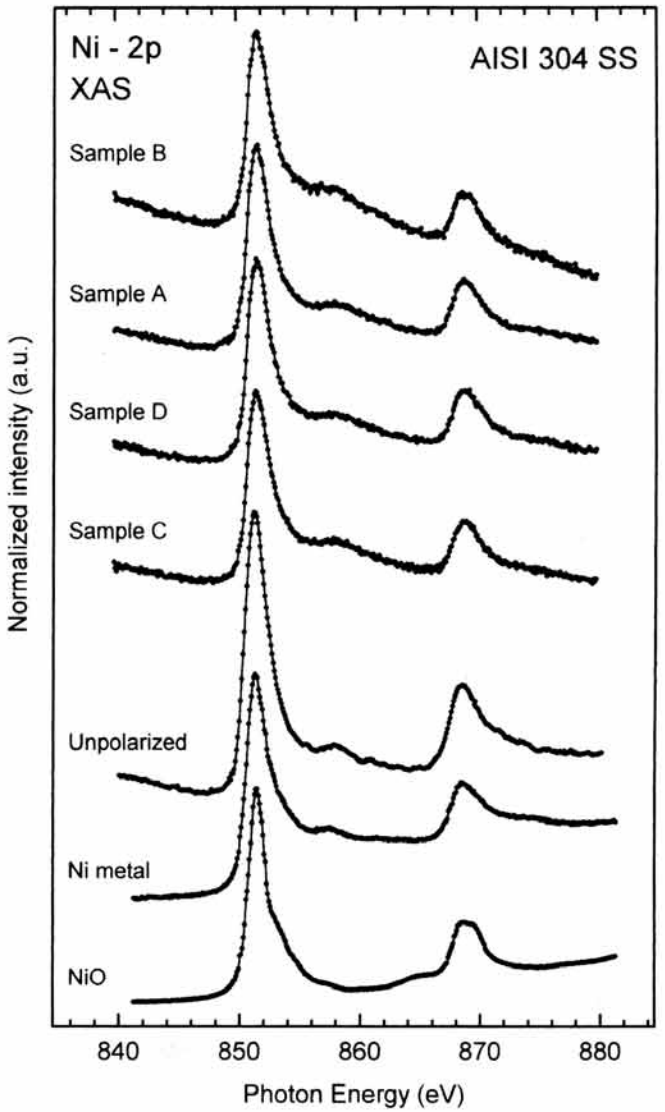

FIG. 7. Ni *2p* soft x-ray absorption spectra for the four polarized AISI 304 SS and the unpolarized AISI 304 SS, Ni metal, and NiO samples. The solid lines through the data points serve as a guide to the eyes.

The spectrum of sample B, however, exhibits a slightly different shape to the other SS samples, with a $2p_{3/2}$ peak more symmetrical and a $2p_{1/2}$ trapezoidal shaped structure similar to the double-peaked structure of the NiO sample. This effect is in agreement with the result of the Fe *2p* AISI 304 SS sample B spectrum, where the highest attack of the substrate due to the highest number of pits in the surface was evidenced. As the spectra shown in Figs. 6 and 7 have been normalized, we can compare the intensities of the $2p_{3/2}$ peak to have an indication of the relative amount of Ni in each sample. The unpolarized samples showed almost twice the Ni intensity of the polarized samples. This effect indicates that Ni depletion probably takes place at the SS surface when the polarization treatment is performed.

The O *1s* soft x-ray absorption spectra of the four polarized AISI 316L SS, the oxidized Cr, the oxidized Fe, and the NiO samples are shown in Fig. 8. The spectra originate from transitions into unoccupied states with O *2p* character hybridized with metal states. Therefore, the structure in the spectra can be qualitatively related to empty bands of primarily metal character. Unfortunately, a quantitative discussion is presently not possible, since a total density of unoccupied states is not available for these compounds. The interpretation of the XAS O *1s* region is in this case less useful than the metal *2p* edges because, when mixtures of oxides are present, the XAS peaks overlap. However, as we mentioned above, qualitative information can be extracted from these data which can complement the results on the transition metal edges. O *1s* spectra can be divided into two regions. The first region, at 525–534 eV, is attributed to oxygen *2p* weight in states of predominantly transition metal *3d* character: the transition metal *3d* band. The second region, 534–545 eV, is attributed to oxygen *p* character hybridized with metal *4s* and *4p* states. The O *1s* spectrum of oxidized Cr in Fig. 8 presents features which are similar to those of Cr_2O_3.[23] The O *1s* spectrum of NiO has the same spectral shape as reported previously.[23] The O *1s* spectrum of oxidized Fe is similar to Fe_2O_3 and to Fe_3O_4 spectra, suggesting a mixture of both chemical compounds in this sample.[14,23]

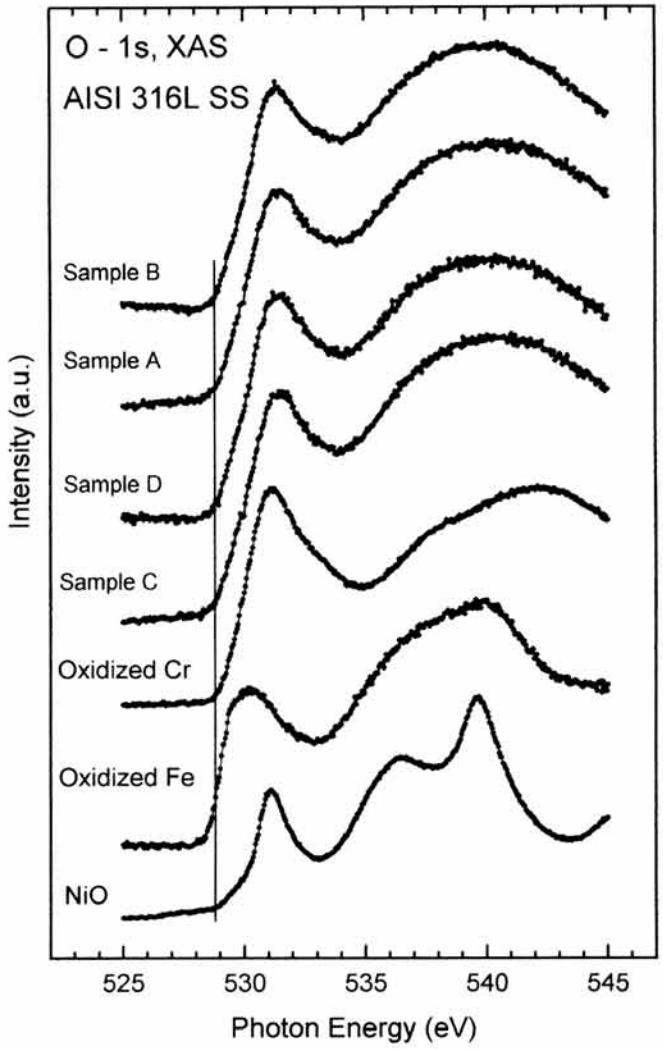

FIG. 8. O *1s* soft x-ray absorption spectra for the four polarized AISI 316L SS, oxidized Cr, oxidized Fe, and NiO samples. The solid lines through the data points serve as a guide to the eyes.

The O *1s* soft x-ray absorption spectra of the four polarized AISI 304 SS are presented in Fig. 9. The polarized SS spectra are similar to oxidized Cr in both regions mentioned above, *3d* band and *4sp* region, although they are not totally identical. A broad structure of the *4sp* band appears in all spectra. This structure can be related to the symmetry set up by the nearest oxygen neighbors, which surround the *3d* transition metal atoms. This broad structure in the SS samples is similar to that of the oxidized Cr and completely different to that of the NiO sample, suggesting no NiO presence in their passive layers. The first region, the *3d* band, of all SS samples is very similar to the oxidized Cr. Nevertheless, there is a shift of the peak onset, indicated by the vertical solid line in Figs. 8 and 9. In the case of the AISI 304 SS, this shift is larger than for the AISI 316L SS samples. The AISI 304 SS sample B shows the largest energy shift. As we can see in Fig. 8, the peak onset of the oxidized Fe *3d* band is located at lower photon energies compared to oxidized Cr *3d* band. This suggests that the observed shifts in the SS samples could be related to the presence of small amounts of oxygen *2p* states hybridized with the Fe *3d* band. As concluded in the case of the Fe *2p* XAS spectra, the presence of Fe oxides has to be excluded, so the observed shift of the peak onset in the O *1s* spectra probably comes from the oxygen *2p* states hybridized to the Fe *3d* band in hydroxides. As we mentioned above, the largest shift is observed for the AISI 304 SS sample B which also exhibits a slightly broader *3d* band. This agrees with the differences observed in Fe *2p* XAS spectrum for this sample, which can be attributed to

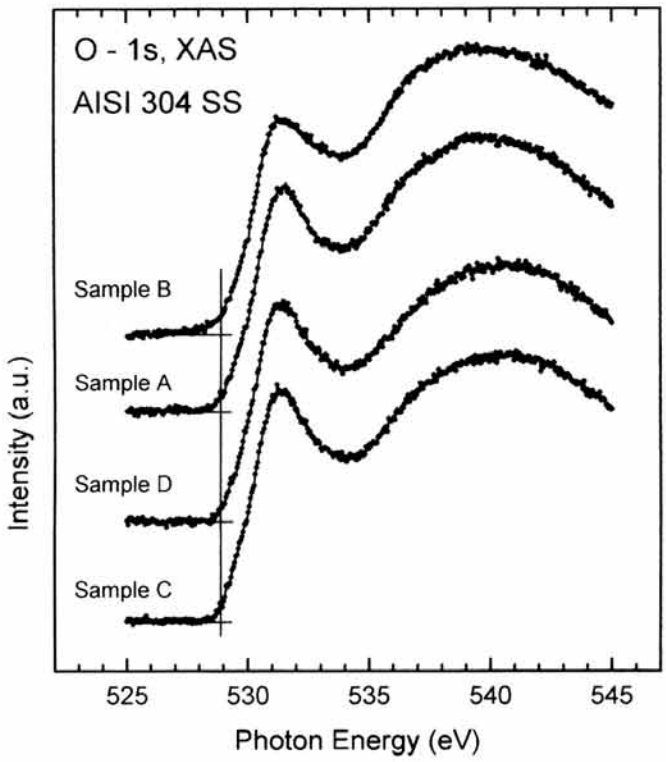

FIG. 9. O *1s* soft x-ray absorption spectra for the four polarized AISI 304 SS samples. The solid lines through the data points serve as a guide to the eyes.

a higher amount of pits in the passive layer of this sample and, therefore, a higher amount of hydroxide compounds, as confirmed by the O *1s* XAS spectra. As mentioned above, the information provided by the O *1s* spectra is complementary to the transition metal *2p* spectra. Therefore, the O *1s* data support the main conclusions reached previously that the passive layer of the SS samples is mainly formed by Cr_2O_3 with some small amounts of hydroxides for the case of the polarized samples. Additionally, the soft x-ray absorption results indicate that the scan rate has an influence on the passive layer electrochemically formed on the material.

IV. CONCLUSIONS

Potentiondynamic polarization curves performed on AISI 316L and 304 SS immersed in a 5% NaCl solution have shown that by increasing the scan rate the breakdown potential also increases and the passivity region becomes larger. In order to obtain more information on the complete passive layer, soft x-ray absorption spectra on both samples, AISI 304 and 316L SS, both at the passivity region and at the pitting region and at two different scan rates were performed. This technique is less surface sensitive than other conventional surface analysis techniques, like XPS or AES, giving more information on the inner part of the passive layer of the material. The XAS spectra at the Cr *2p* edges exhibit for all SS samples, polarized and unpolarized, similar spectral features to that of Cr_2O_3, with almost no metallic Cr signal from the substrate. The XAS spectra at the Fe and Ni *2p* edges show similar spectral shapes to that of metallic Fe and Ni, respectively, suggesting almost no Fe and Ni oxides nor hydroxide incorporation into the passive layer. However, the AISI 304 SS sample polarized at the lowest scan rate and at the highest polarization potential, sample B, presents slight differences that may be attributed to a higher content of Fe hydroxide and Ni oxide due to a higher amount of pits as observed by the optical microscope. The Ni *2p* spectra suggest also that the anodic polarization treatment produces Ni depletion at the surface, as deduced by taking into account the Ni intensity ratios. The XAS O *1s* spectra support the main conclusions obtained with the transition metal edges spectra. These results indicate that the scan rate has an influence on the passive layer electrochemically formed on the material.

ACKNOWLEDGMENTS

This work has been supported by the Spanish Interministerial Science and Technology Commission (CICYT) under Project No. QUI97-0666-C02-01, and by the BESSY Contract No. CHGE-CT93-0027 of the Human Capital and Mobility Program of the EU. Technical assistance by BESSY-staff is gratefully acknowledged.

REFERENCES

1. A.R. Brooks, C.R. Clayton, K. Doss, and Y.C. Lu, J. Electrochem. Soc. **133**, 2459 (1986).
2. G. Lorang, M. Da Cunha Belo, A.M.P. Simoes, and M.G.S. Ferreira, J. Electrochem. Soc. **141**, 3347 (1994).
3. I. Olefjord and L. Wegrelius, Corros. Sci. **31**, 89 (1990).
4. H.J. Mathieu and D. Landolt, Corros. Sci. **26**, 547 (1986).
5. R. Kirchheim, B. Heine, H. Fischmeister, S. Hofmann, H. Knote, and U. Stolz, Corros. Sci. **29**, 899 (1989).
6. K. Asami, K. Hashimoto, and S. Shimodaira, Corros. Sci. **18**, 151 (1978).
7. V. Maurice, W.P. Yang, and P. Marcus, J. Electrochem. Soc. **143**, 1182 (1996).
8. S.C. Tjong, R.W. Hoffmann, and E.B. Yeager, J. Electrochem. Soc. **129**, 1662 (1982).
9. P. Brüesch, K. Müller, A. Atrens, and H. Neff, Appl. Phys. A **38**, 1 (1985).
10. G. Hultquist, C. Leygraf, and D. Brune, J. Electrochem. Soc. **131**, 1773 (1984).
11. D.R. Penn, Phys. Rev. B **13**, 5248 (1976).
12. M. Abbate, J.B. Goedkoop, F.M.F. de Groot, M. Grioni, J.C. Fuggle, S. Hofmann, H. Petersen, and M. Sacchi, Surf. Interface Anal. **18**, 65 (1992).
13. S.L.M. Schroeder, Solid State Commun. **98**, 405 (1996).
14. J.C. Fuggle and J.E. Inglesfield, in *Unoccupied Electronic States* (Springer, Berlin, 1991).
15. R.D. Leapman, L.A. Grunes, and P.L. Fejes, Phys. Rev. B **26**, 614 (1972).
16. Z.Y. Wu, S. Gota, F. Joliet, M. Pollak, M. Gautier-Soyer, and C.R. Natoli, Phys. Rev. B **55**, 2570 (1997).

17. J. McBreen, W. E. O'Grady, G. Tourillon, E. Dartyge, and A. Fontaine, J. Electroanal. Chem. **307**, 229 (1991).
18. M. Abbate, F. M. F. de Groot, J. C. Fuggle, A. Fujimori, Y. Tokura, Y. Fujishima, O. Strebel, M. Domke, G. Kaindl, J. van Elp, B. T. Thole, G. A. Sawatzky, M. Sacchi, and N. Tsuda, Phys. Rev. B **44**, 5419 (1991).
19. F. M. F. de Groot, J. C. Fuggle, B. T. Thole, and G. A. Sawatzky, Phys. Rev. B **42**, 5459 (1990).
20. F. M. F. de Groot, Z. W. Hu, M. F. López, G. Kaindl, F. Guillot, and M. Tronc, J. Chem. Phys. **101**, 6570 (1994).
21. L. Soriano, M. Abbate, F. M. F. de Groot, D. Alders, J. C. Fuggle, S. Hofmann, H. Petersen, and W. Braun, Surf. Interface Anal. **20**, 21 (1993).
22. P. J. Weijs, G. Wiech, W. Zahorowski, W. Speier, J. B. Goedkoop, M. Czyzyk, J. F. van Acker, E. vanLeuken, R. A. de Groot, G. van der Laan, D. D. Sarma, L. Kumar, K. H. J. Buschow, and J. C. Fuggle, Phys. Scripta **41**, 629 (1990).
23. F. M. F. de Groot, M. Grioni, J. C. Fuggle, J. Ghijsen, G. A. Sawatzky, and H. Petersen, Phys. Rev. B **40**, 5715 (1989).